Construction and Building Materials 281 (2021) 122570

Contents lists available at ScienceDirect

Construction and Building Materials

journal homepage: www.elsevier.com/locate/conbuildmat

Dynamic splitting tensile bond behavior of new-to-old concrete interfaces

Bo Hu [a,b,*], Teng-Fei Meng [a], Yuan Li [a], Dao-Zhong Li [c], Long Chen [d]

[a] College of Civil Engineering, Hefei University of Technology, Hefei 230009, PR China
[b] Anhui Key Laboratory of Civil Engineering Structures and Materials, Hefei University of Technology, Hefei 230009, PR China
[c] China Hefei State Construction International Investment and Development Company Limited, Hefei 230000, PR China
[d] Hefei Cement Research and Design Institute Corporation Limited, Hefei 230051, PR China

HIGHLIGHTS

- The strain rate has significant effects on tensile bond behavior of interfaces.
- The surface roughness and interface age have little effects on bond strength.
- A new dynamic increase factor of the tensile strength is proposed for interfaces.

ARTICLE INFO

Article history:
Received 14 August 2020
Received in revised form 10 January 2021
Accepted 30 January 2021

Keywords:
New-to-old concrete interface
Splitting tensile test
Strain-rate effect
Bond strength
Dynamic increase factor

ABSTRACT

New-to-old concrete interfaces, which widely exist in concrete structures, are commonly regarded as weak links. Hence, many researchers have studied the splitting tensile bond behavior of concrete interfaces. However, these studies were focused on the behavior under quasi-static loading. Concrete interfaces may suffer blast and/or impact loading during their service lives. Therefore, this paper experimentally investigated the dynamic splitting tensile bond behavior of concrete interfaces. For comparison, a quasi-static splitting tensile test was also carried out. A total of 46 splitting tensile cylinders were tested. Test parameters included three strain rates (10^{-6}, 0.63 and 1.58/s), two levels of average roughness (1.2 and 2.4 mm) and two interface ages (60 and 120 days). Experimental results show that influences of the strain rate on failure modes, compressive load-deformation curves, absorption energy and splitting tensile bond strength of specimens are significant. The surface roughness and interface age have little effects on splitting tensile bond strength. Existing formulas for the dynamic increase factor of the tensile strength of concrete-like materials cannot be used for concrete interfaces. Consequently, a new formula for the dynamic increase factor of the splitting tensile bond strength of concrete interfaces is finally proposed.

1. Introduction

New-to-old concrete interfaces widely exist in concrete structures, such as long and large concrete structures, monolithic precast concrete structures and repaired concrete structures, where concrete is usually poured at different times. Due to the difference in performance between old and new concrete, a concrete interface is commonly regarded as a weak link of a concrete structure [1,2]. On the other hand, concrete is a kind of material that is easy to crack and fail under tension. Therefore, for a concrete interface, an important issue is its tensile bond behavior.

There are two categories of methods for testing the tensile bond behavior of concrete interfaces. The first category includes direct tension [1] and pull-off [2–12] tests, in which a specimen is tested under tension and the interface is directly subjected to tensile loading. For this category of test methods, the specimen needs to be carefully aligned in the loading direction. Otherwise, a large scatter in experimental results may be introduced due to the misalignment. Moreover, cohesive failure may happen, which will result in a less estimation for the tensile bond strength of the concrete interface. The second category contains flexural [11,13] and splitting [2,9,12–23] tests, where a specimen is tested under bending or compression and the interface is indirectly subjected

* Corresponding author at: College of Civil Engineering, Hefei University of Technology, Hefei 230009, PR China.
E-mail address: bohu@hfut.edu.cn (B. Hu).

https://doi.org/10.1016/j.conbuildmat.2021.122570
0950-0618/

to tension. In the flexural test, the interface is partially in compression and partially in tension during flexural loading. The non-uniform stress distribution will cause a greater estimation for the tensile bond strength of the concrete interface. In the splitting test, compressive loads are applied along the upper and lower boundary lines of the interface of a cylindrical or cubic specimen. Then, uniform tensile stress is induced on the diametric plane of the interface. Due to the advantage, the splitting test has been widely used to investigate the tensile bond behavior of concrete interfaces [2,9,12–23].

Before new concrete is cast, the substrate surface of old concrete needs to be treated. Commonly used methods for treating the surface include wire-brushing [2,4,5,7,9,13,17–19], grooving [12,17–19], hand-scrubbing [7], sand-blasting [4,5,7,12,17–19], drilling [13,17,18], hand-chiseling [14], chipping [4–6,23] and shot blasting [7]. Existing test results [4,5,7,17–19] showed that the mentioned surface treatment methods have significant influences on the splitting tensile bond strength of concrete interfaces. Surface treatment aims to create a rough surface and then improve the bond performance between old and new concrete. However, the rough surface by a commonly used method is produced after old concrete is cured. At that time, old concrete has certain hardness and the produced surface roughness largely depends on the levels of manual operation and/or machine performance in the process of surface treatment. Within this condition, it is difficult to quantitatively control the roughness. Thus, it is also difficult to quantitatively evaluate the effect of the surface roughness produced by the commonly used method. Recently, Hu et al. [24] created a rough surface through a formwork with rectangular strips in the process of casting old concrete. By the new method, surface roughness could be quantitatively designed and controlled according to the width and spacing of the rectangular strips of the formwork.

The application of bonding agents is another way to improve the bond performance of concrete interfaces. Tests conducted by Júlio et al. [5], Bonaldo et al. [6], He et al. [9] and Huang et al. [22] indicated that bonding agents enhance the splitting tensile bond strength between old and new concrete and the choice of bonding agents has a significant effect. Nevertheless, Júlio et al. [5] also pointed out that the bonding agent does not improve the splitting tensile bond strength if the roughness of the substrate surface has been adequately increased by the surface treatment method.

Old and new concrete, which bond with each other at an interface, have different ages. Hence, Santos and Júlio's [16] conducted a splitting test to investigate the effect of age differences (i.e., 28, 56 and 84 days) between old and new concrete on the tensile bond behavior. The test results demonstrated that the splitting tensile bond strength increases as the age difference increases. On the other hand, He et al. [9], Tayeh et al. [17], Abo Sabah et al. [12] and Li [3] experimentally studied the influences of interface ages (i.e., 7 and 28 days in [9], 3, 7 and 28 days in [17], 7, 28, and 90 days in [12] and 28 days and 1 year in [3]). The experimental results indicated that, with the increase in the interface age, the splitting tensile bond strength significantly increases when the age is not more than 28 days but slightly increases when the age is beyond 28 days.

Besides, Gadri and Guettala [13] and Huang et al. [22] examined the effects of strength grades of old and new concrete on the tensile bond performance of interfaces, respectively. They concluded that the splitting tensile bond strength increases as the strength grade of old or new concrete increases. Santos and Júlio's [16] test results showed that the difference of stiffness between old and new concrete has important effects on the splitting tensile bond strength and failure modes of new-to-old concrete interfaces. In addition, Gao et al. [21] experimentally found that the higher temperature also has a great influence on the splitting tensile bond behavior between old and new concrete.

However, the existing splitting tensile tests were focused on the quasi-static bond behavior of concrete interfaces. Concrete interfaces may suffer blast and impact loading during their service lives. It is necessary to study the dynamic splitting tensile bond behavior between old and new concrete. Therefore, this paper employed the split Hopkinson pressure bar (SHPB) to apply impact loading and conducted a dynamic splitting tensile test of new-to-old concrete interfaces. For comparison, a quasi-static splitting tensile test was also conducted. Effects of the strain rate, the surface roughness and the interface age on the splitting tensile bond behavior of concrete interfaces were investigated.

2. Test program

2.1. Specimen characterization

In this test program, a total of 46 splitting tensile cylinders were prepared and examined, as list in Table 1. Three loading rates, which include one quasi-static loading rate (0.01 kN/s) and two dynamic loading rates (7.77 and 14.63 m/s), were used to investigate the effect of the strain rate on the splitting tensile bond behavior of concrete interfaces. The quasi-static loading rate of 0.01 kN/s was chosen to achieve the quasi-static strain rate of 10^{-6}/s, which is suggested by *fib* Model Code 2010 [25]. In a SHPB test, the concrete interface will not be split if the dynamic loading rate is very low. When the dynamic loading rate becomes very high, the old concrete substrate and new concrete layer will be severely damaged, resulting in inaccurate interfacial tensile bond strength. Therefore, two moderate dynamic loading rates, i.e., 7.77 and 14.63 m/s, were selected for the SHPB test. Under the quasi-static loading rate of 0.01 kN/s, 16 specimens were tested. Under the dynamic loading rates of 7.77 and 14.63 m/s, 14 and 16 specimens were tested, respectively.

The cylinder specimens under different loading rates had the same diameter and height. Due to the pressure bars of the SHPB have the diameter of 74 mm, all the cylinder specimens were 70 mm in diameter and 60 mm in height. On the surface of each old concrete substrate, two parallel rectangular grooves were arranged to create a rough surface. The grooves had the width of 14 mm and the spacing of 14 mm. Two depths, i.e., 3 and 6 mm, were used to produce two levels of surface roughness. The geometry of the cylinder specimens is shown in Fig. 1. In *fib* Model Code 2010 [25], an equation is suggested to quantify the roughness of a concrete substrate surface as follows:

$$R_a = \frac{1}{D_s}\int_0^{D_s} y(x)\mathrm{d}x \tag{1}$$

where R_a is the average roughness; D_s is the diameter of the specimen; and $y(x)$ is the profile height at position x. According to Eq. (1), the average roughness of concrete interfaces with the groove depths of 3 and 6 mm were 1.2 and 2.4 mm, respectively.

Concrete interfaces are more likely to be subjected to dynamic loading during their service lives. At that time, ages of concrete interfaces are usually more than 28 days. Thus, two interface ages, i.e., 60 and 120 days, were used. Since a concrete interface was formed by pouring new concrete on old concrete, the interface age was equal to the age of new concrete.

2.2. Concrete mixtures

In this subsection, three Chinese codes for structural design, i.e., GB 50666-2011 [26], JGJ 1-2014 [27], and GB 50367-2013 [28], were first utilized to determine the strength grades of old and

Table 1
Test specimens and results.

Specimen[a]	Average roughness (mm)	Interface age (days)	Loading rate		Strain rate		Failure mode	Splitting tensile bond strength		
			Individual value	Average value	Individual value (1/s)	Average value (1/s)		Individual value (MPa)	Average value (MPa)	COV (%)
SPR1A1S-1	1.2	60	0.01 kN/s	0.01 kN/s	10^{-6}	10^{-6}	II	3.05	3.04	8.2
SPR1A1S-2	1.2	60	0.01 kN/s		10^{-6}		I	2.71		
SPR1A1S-3	1.2	60	0.01 kN/s		10^{-6}		II	3.10		
SPR1A1S-4	1.2	60	0.01 kN/s		10^{-6}		II	3.31		
SPR2A1S-1	2.4	60	0.01 kN/s		10^{-6}		IV	2.84	3.11	13.9
SPR2A1S-2	2.4	60	0.01 kN/s		10^{-6}		IV	3.35		
SPR2A1S-3	2.4	60	0.01 kN/s		10^{-6}		II	3.60		
SPR2A1S-4	2.4	60	0.01 kN/s		10^{-6}		IV	2.67		
SPR1A2S-1	1.2	120	0.01 kN/s		10^{-6}		IV	2.44	3.26	17.9
SPR1A2S-2	1.2	120	0.01 kN/s		10^{-6}		IV	3.35		
SPR1A2S-3	1.2	120	0.01 kN/s		10^{-6}		V	3.48		
SPR1A2S-4	1.2	120	0.01 kN/s		10^{-6}		IV	3.80		
SPR2A2S-1	2.4	120	0.01 kN/s		10^{-6}		IV	3.23	3.24	14.6
SPR2A2S-2	2.4	120	0.01 kN/s		10^{-6}		IV	2.60		
SPR2A2S-3	2.4	120	0.01 kN/s		10^{-6}		II	3.71		
SPR2A2S-4	2.4	120	0.01 kN/s		10^{-6}		IV	3.42		
SPR1A1V1-1	1.2	60	7.80 m/s	7.77 m/s	0.73	0.63	III	4.88	4.59	26.9
SPR1A1V1-2	1.2	60	7.74 m/s		0.50		II	3.88		
SPR1A1V1-3	1.2	60	7.80 m/s		0.94		II	6.19		
SPR1A1V1-4	1.2	60	7.86 m/s		0.45		I	3.40		
SPR2A1V1-1	2.4	60	7.82 m/s		0.87		II	5.89	4.59	27.9
SPR2A1V1-2	2.4	60	7.76 m/s		0.44		II	3.33		
SPR2A1V1-3	2.4	60	7.81 m/s		0.58		II	4.54		
SPR1A2V1-1	1.2	120	7.73 m/s		0.52		III	4.47	4.67	21.2
SPR1A2V1-2	1.2	120	7.73 m/s		0.76		I	5.99		
SPR1A2V1-3	1.2	120	7.79 m/s		0.46		II	3.61		
SPR1A2V1-4	1.2	120	7.75 m/s		0.59		II	4.60		
SPR2A2V1-1	2.4	120	7.76 m/s		0.58		IV	4.21	4.73	17.6
SPR2A2V1-2	2.4	120	7.69 m/s		0.67		IV	4.28		
SPR2A2V1-3	2.4	120	7.69 m/s		0.77		IV	5.69		
SPR1A1V2-1	1.2	60	14.51 m/s	14.63 m/s	2.03	1.58	II	8.51	7.95	9.2
SPR1A1V2-2	1.2	60	14.60 m/s		1.52		II	6.96		
SPR1A1V2-3	1.2	60	14.51 m/s		2.24		IV	8.47		
SPR1A1V2-4	1.2	60	14.56 m/s		1.47		III	7.85		
SPR2A1V2-1	2.4	60	14.47 m/s		1.55		II	9.61	8.60	10.4
SPR2A1V2-2	2.4	60	14.49 m/s		1.75		V	8.52		
SPR2A1V2-3	2.4	60	14.45 m/s		1.37		V	7.46		
SPR2A1V2-4	2.4	60	14.49 m/s		1.87		II	8.81		
SPR1A2V2-1	1.2	120	14.73 m/s		1.55		III	6.97	7.73	9.9
SPR1A2V2-2	1.2	120	14.71 m/s		1.36		III	7.18		
SPR1A2V2-3	1.2	120	15.02 m/s		1.76		III	8.48		
SPR1A2V2-4	1.2	120	15.04 m/s		1.36		II	8.28		
SPR2A2V2-1	2.4	120	14.53 m/s		1.36		V	7.57	7.44	5.0
SPR2A2V2-2	2.4	120	14.71 m/s		1.24		V	7.29		
SPR2A2V2-3	2.4	120	14.56 m/s		1.22		IV	7.02		
SPR2A2V2-4	2.4	120	14.62 m/s		1.64		V	7.89		

[a]*Note:* SP represents the splitting tensile test. R1 and R2 denote the surface roughness and mean the average roughness of 1.2 and 2.4 mm, respectively. A1 and A2 denote the interface age and correspond to 60 and 120 days, respectively. S represents the quasi-static loading rate of 0.01 kN/s and V1 and V2 mean the dynamic loading rates of 7.77 and 14.63 m/s, respectively. The final numbers indicate that the same specimens were tested three or four times.

new concrete. Then, Chinese code JGJ 55-2011 [29] was used for concrete mixtures.

For a long and large concrete structure, Chinese code GB 50666-2011 [26] specifies that concrete in post-cast strips should be one strength grade higher than existing concrete and the latter usually has a strength grade of not lower than C20. For a monolithic precast concrete structure, Chinese specification JGJ 1-2014 [27] suggests that precast concrete must have a strength grade of not smaller than C30 and cast-in-site concrete should not have a lower strength grade than precast concrete. For a repaired concrete structure, Chinese specification GB 50367-2013 [28] stipulates that repairing concrete must have a strength grade of not less than C20 and should be one strength grade higher than old concrete. Therefore, C30 and C40 strength grades were employed for old and new concrete in this experimental program, respectively.

According to Chinese code JGJ 55-2011 [29], mix proportions in Table 2 were adopted to manufacture old and new concrete. Due to the grooves were 14 mm in width and spacing, the selected maximum gravel size was 10 mm for coarse aggregate. The compressive strength, f_c, of 150 mm cube samples of concrete was assessed on the testing days. For each concrete type and age, the average value of f_c of three cubes was obtained, as listed in Table 2.

2.3. Specimen preparation

C30 concrete was first cast. Before pouring C30 concrete, formworks were fabricated. A formwork was composed of a PVC tube, a PVC base plate, a PVC division plate and a PVC stiffened plate, as shown in Fig. 2(a). The tube had the internal diameter of 70 mm and the height of 80 mm. The division and stiffened plates had the same height as the tube. One surface of the division plate had the width of 70 mm, which is the same as the internal diameter of the tube. Two parallel PVC strips were attached on the surface. The depths, width and spacing of the strips were the same

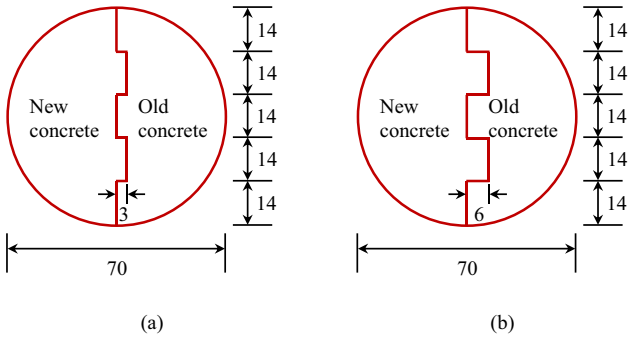

Fig. 1. Geometry of splitting tensile specimens (in mm): (a) specimen with the average roughness of 1.2 mm; and (b) specimen with the average roughness of 2.4 mm.

Table 2
Mix proportions and compressive strength of concrete.

Type		Old concrete	New concrete
Grade		C30	C40
Mix proportion	P.O 42.5 Portland cement	0.82	0.77
	Medium-sized river sand	1.74	1.24
	Coarse aggregate	2.30	1.86
	Type I fly ash	0.08	0.08
	S95 slag powder	0.10	0.15
	Potable water	0.48	0.36
	PY-I pumping admixture	0.016	–
	PCA-I polycarboxylate superplasticizer	–	0.015
Compressive strength f_c (MPa)	60 days[a]	55.2 (90 days[b])	61.9 (60 days[c])
	120 days[a]	56.0 (150 days[b])	62.8 (120 days[c])

[a]The number of days denotes the age of concrete interfaces.
[b]The number of days denotes the age of old concrete.
[c]The number of days denotes the age of new concrete.

as those of the grooves. Another surface of the division plate was bonded to the stiffened plate. The stiffened plate was used to prevent the division plate from shifting during the pouring process of old concrete. The PVC tubes, plates and strips were pasted with a cyanoacrylate adhesive. After the preparation of formworks, C30 concrete was poured into the formworks to fabricate old concrete substrates.

After 10 days, the old concrete substrates were moved out of the formworks and placed in a laboratory for 20 days, as shown in Fig. 2(b). Before casting C40 concrete, the surface of each old concrete substrate was cleaned and pre-wetted. After that, the old concrete substrate was placed in one half of a PVC tube with a PVC base plate. The PVC tube was also 70 mm in internal diameter and 80 mm in height. Then, C40 concrete was poured into the other half of the tube to form a new concrete layer, as shown in Fig. 2(c). Thus, an old concrete substrate and a new concrete layer composed a splitting tensile specimen.

Ten days later, the splitting tensile specimens were taken out from the tubes, as shown in Fig. 2(d). After 28 days, the two ends of each specimen were cut, so that the height of each specimen was 60 mm, as shown in Fig. 2(e). When the ages of the new concrete layers achieved 60 and 120 days, the specimens were tested.

2.4. Quasi-static test

A 100 kN electronic universal testing machine (WDW-100) was used to test the specimens under quasi-static loading. The compressive loading rate was a constant and equal to 0.01 kN/s. The corresponding strain rate was about 10^{-6}/s. Before testing each specimen, diametral lines on the two circular end surfaces of the specimen were drawn along the interface. Two pieces of plywood, which were 3.0 mm in thickness and 20 mm in width and have a slightly longer length than the specimen, were employed as bearing strips in accordance with Chinese code GB/T 50081-2002 [30]. The two plywood strips were placed along the centers of the upper and lower bearing blocks of the testing machine, respectively. Then, the specimen was placed between the two plywood strips and aligned, so that the diametral lines were perpendicular to the plywood strips and consistent with the loading direction. During testing, the quasi-static compressive load, $P_s(t)$, and deformation, $\Delta u_s(t)$, of each specimen were recorded at the same time. The test was finished when the specimen failed. Fig. 3(a) shows the setup of the quasi-static test.

Based on the splitting tensile test principle, the quasi-static splitting tensile bond strength, $f_{s,st}$, of a new-to-old interface was determined by the following expression [31]:

$$f_{s,st} = \frac{2P_{s,max}}{\pi D_s H_s}\left[1 - \left(\frac{b}{D_s}\right)^2\right]^{3/2} \tag{2}$$

where, $P_{s,max}$ is the maximum applied quasi-static compressive load; H_s is the height of the specimen; and b is the width of the strips.

2.5. SHPB test

A SHPB system was employed to examine the specimens under dynamic loading. Fig. 3(b) and (c) depicts the setup and configuration of the SHPB test. The bars were made of alloy steel, which has the Young's modulus, E, of 210 GPa and the wave propagation velocity, C_0, of 5172 m/s. Before testing each specimen, vaseline was evenly smeared near the two new-to-old concrete boundary lines on the cylindrical surface of the specimen. Then, the two boundary lines were contacted with the incident and transmission bars, respectively. The incident, reflected and transmitted strains, $\varepsilon_i(t)$, $\varepsilon_r(t)$ and $\varepsilon_t(t)$, were measured by two strain gauges mounted on the bars, as plotted in Fig. 3(c). Compressed air was used to launch the striker bar, so that two average striker impact speeds, i.e., 7.77 and 14.63 m/s, were induced. The corresponding two strain rates were 0.63 and 1.58/s.

In accordance with the one-dimensional wave theory and the splitting tensile test principle, the dynamic compressive load, $P_d(t)$, deformation, $\Delta u_d(t)$, splitting tensile bond strength, $f_{d,st}$, and strain rate, $\dot{\varepsilon}$, of a new-to-old interface in the SHPB test were calculated by the following expressions:

$$\sigma_t(t) = E\varepsilon_t(t) \tag{3}$$

$$P_d(t) = \frac{\pi D^2}{4}\sigma_t(t) \tag{4}$$

$$u_1(t) = C_0\int_0^T (\varepsilon_i(t) - \varepsilon_r(t))dt \tag{5}$$

$$u_2(t) = C_0\int_0^T \varepsilon_t(t)dt \tag{6}$$

$$\Delta u_d(t) = u_1(t) - u_2(t) \tag{7}$$

$$f_{d,st} = \frac{2P_{d,max}}{\pi D_s H_s} \tag{8}$$

$$\dot{\varepsilon} = \frac{f_{d,st}}{T_0 E_s} \tag{9}$$

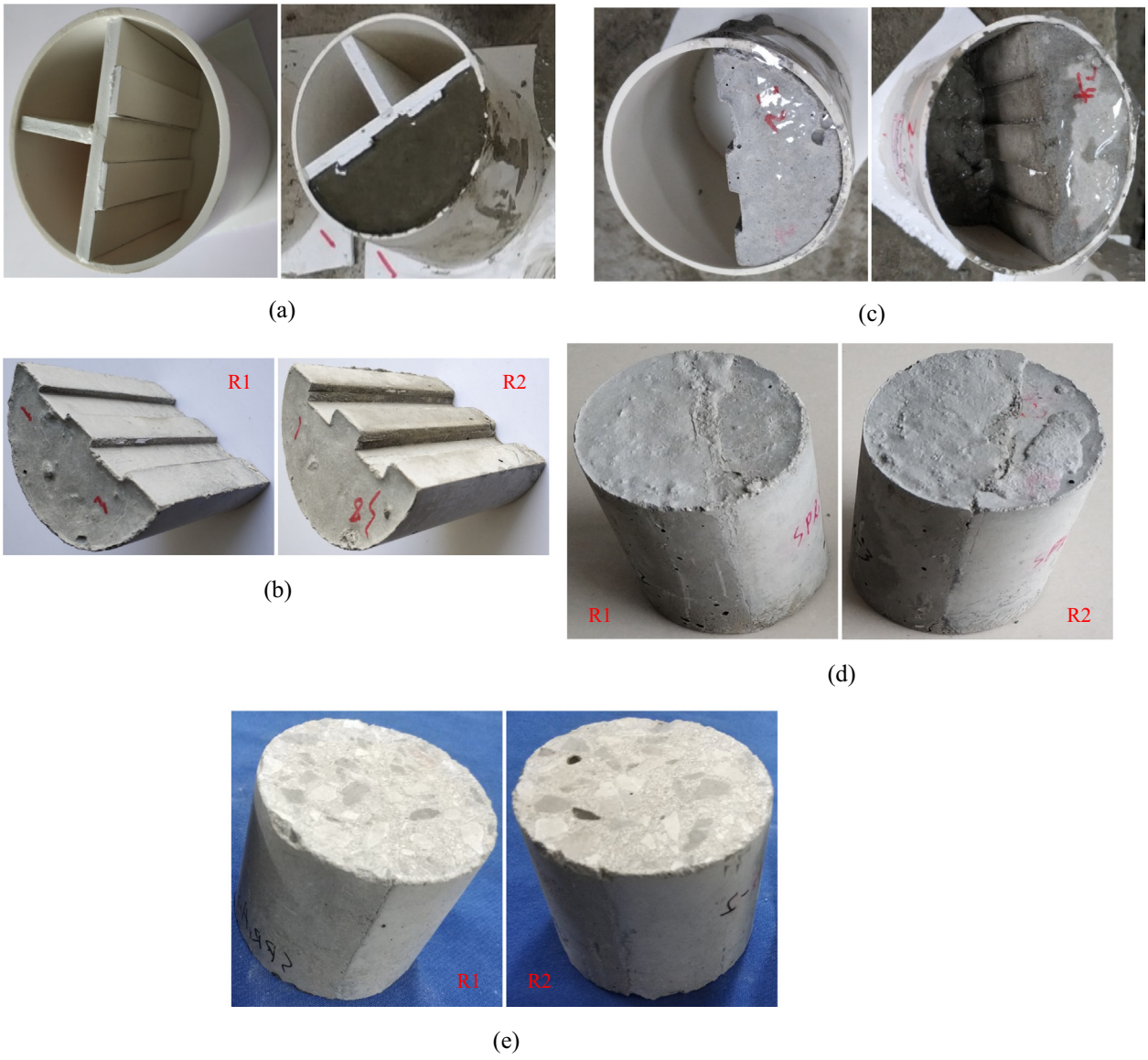

Fig. 2. Formworks and cylinder specimens: (a) formwork for casting old concrete; (b) old concrete semicylinders; (c) formwork for casting new concrete; (d) cylinder specimens before cutting; and (e) cylinder specimens after cutting. (Note: the new concrete semicylinder is on the left and the old concrete semicylinder is on the right in each figure of (d) and (e).)

where $\sigma_t(t)$ is the transmitted stress; $u_1(t)$ and $u_2(t)$ are the displacements of the ends of the incident and transmission bars contacted with the specimen, respectively; $P_{d,max}$ is the maximum applied dynamic compressive load; T_0 is the time lag between the start of the transmitted stress wave and the maximum transmitted stress; and E_s is the elastic modulus of the specimen. For a concrete interface specimen, stress waves propagate in both old and new concrete during dynamic loading. The effects of the elastic moduli of both old and new concrete should be considered when determining E_s. Thus, E_s was assumed to be equal to the average value of the elastic moduli of old and new concrete in this experimenal program. The elastic moduli of old and new concrete were estimated through the compressive strength, f_c, measured in Section 2.2. The formula, $4700\sqrt{f'_c}$, suggested in ACI 318 M–05 [32] was employed for the estimation, where f'_c is the cylinder compressive strength of concrete and was approximately determined by $0.79f_c$ according to *fib* Model Code 2010 [25].

To check the validity of the SHPB test, the following stress equilibrium equation was employed,

$$\sigma_i(t) + \sigma_r(t) = \sigma_t(t) \tag{10}$$

where $\sigma_i(t)$ and $\sigma_r(t)$ are the incident and reflected stresses, respectively. Fig. 4 shows a typical set of stress equilibrium of the specimen under the striker impact speed of 7.77 m/s. It implies that the SHPB test is valid.

3. Test results and analysis

3.1. Failure modes

Fig. 5 shows failure modes of specimens. It can be seen that typical splitting failure occurs at the interface of each specimen. For a splitting tensile cylinder specimen under loading, compressive stress appears at two bearing ends of the specimen, while tensile

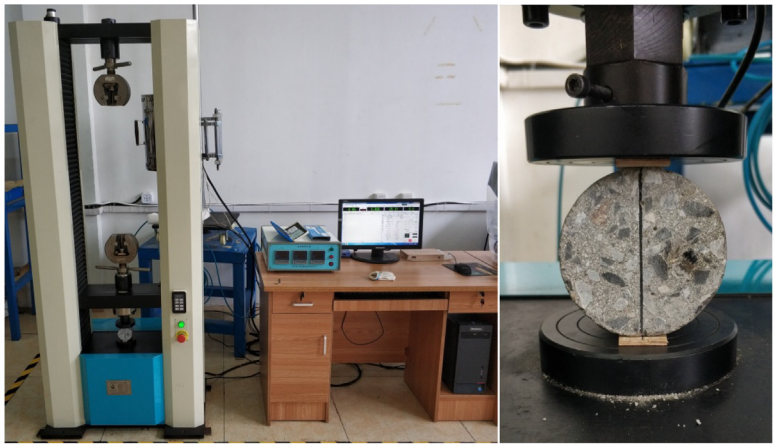

(a)

(b)

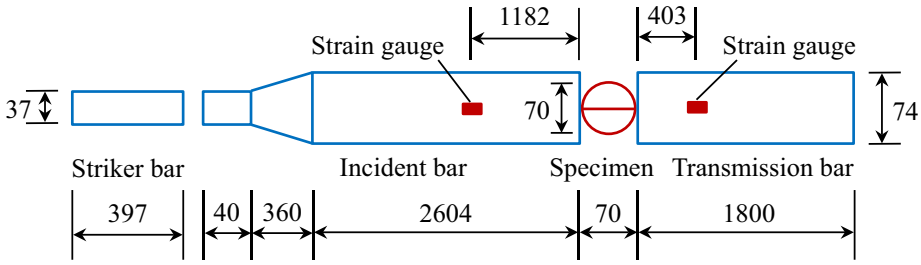

(c)

Fig. 3. Test setups and configuration: (a) quasi-static test setup; (b) SHPB test setup; and (c) configuration of the SHPB test (in mm).

stress arises in the middle of the specimen. In the middle of each specimen, the old concrete substrate has one bulge and the new concrete layer has two bulges, which compose the main part of the new-to-old bond interface subjected to the tensile stress. According to the extent of splitting failure of specimens, five failure modes are observed as follows:

Ⅰ—the specimen is split at the interface, the old concrete bulge in the middle remains almost intact and the new concrete bulges in the middle are partially pulled off, as shown in Fig. 5(a);

Ⅱ—the specimen is split at the interface, the old concrete bulge in the middle remains almost intact and the new concrete bulges in the middle are completely pulled off, as shown in Fig. 5(b);

Ⅲ—the specimen is split at the interface and both the old concrete bulge and the new concrete bulges in the middle are partially pulled off, as shown in Fig. 5(c);

Ⅳ—the specimen is split at the interface, the old concrete bulge in the middle is partially pulled off and the new concrete bulges in the middle are completely pulled off, as shown in Fig. 5(d);

and Ⅴ—the specimen is split at the interface and both the old concrete bulge and the new concrete bulges in the middle are completely pulled off, as shown in Fig. 5(e).

Table 1 lists the observed failure modes of all the splitting tensile specimens. It is clear that, under each strain rate, failure mode Ⅰ or Ⅱ tends to take place in the specimens with the average roughness of 1.2 mm and the interface age of 60 days. When the average roughness is 2.4 mm and/or the interface age is 120 days, failure mode Ⅳ is inclined to occur under the strain rates of 10^{-6} and 0.63/s, while failure mode Ⅲ or Ⅴ is more likely to occur under the strain rate of 1.58/s. It indicates that the tensile damage of the old concrete substrates becomes more serious with the

increases in the surface roughness and interface age. On the other hand, failure modes I and III only happen in the specimens with the average roughness of 1.2 mm. When the average roughness becomes 2.4 mm, failure mode II, IV, or V occurs. It means that the new concrete layers suffer more tensile damage with the increase in the surface roughness. However, the interface ages of 60 and 120 days have little effects on the damage of the new concrete layers.

When the loading type changes from quasi-static loading to dynamic loading, it seems that both the old concrete substrates and the new concrete layers does not necessarily go through more splitting damage. It might be attributed to two reasons. One is that the two dynamic loading rates used in this test program are not great and does not cause very serious damage of the specimens. The other is that under dynamic loading, the whole specimen is quickly split before some of the concrete bulges have not yet been partially or completely pulled off. When the strain rate increases from 0.63/s to 1.58/s, the main failure modes change from II and IV to II and V. It demonstrates that the old concrete substrates undergo more tensile damage with the increase in the dynamic strain rate and the new concrete bulges are almost fully pulled off under both the two dynamic strain rates.

3.2. Compressive load-deformation curves

Fig. 6(a) describes the recorded compressive load-deformation curves in the quasi-static test. Note that the compressive deformation in each curve contains not only the compressive deformation of the specimen but also the compressive deformation of the two plywood strips. However, the compressive load in each curve is consistent with that applied to the specimen. From Fig. 6(a), it can be seen that the average roughness and interface age have no significant effects on the maximum compressive loads of specimens under the strain rate of 10^{-6}/s.

According to Eq. (4) and (7), the dynamic compressive load and deformation of each specimen in the SHPB test were calculated, respectively. Then, the compressive load-deformation curves of specimens were obtained, as shown in Fig. 6(b) and (c). For each specimen under the strain rates of 0.63 and 1.58/s, the compressive load slowly increases at first as the compressive deformation increases. When the compressive deformation approximately exceeds 0.1 mm, the compressive load quickly increases. Before the compressive load achieves the maximum value, the enhancement of the compressive load becomes slower. After exceeding the maximum value, the compressive load decreases with the increase in the compressive deformation. When the compressive deformation reaches the maximum value, the compressive load and deformation decrease at the same time and the specimen goes through recovery. When the compressive load decreases to 0 kN, the residual compressive deformation appears.

When the strain rate increases from 10^{-6}/s to 0.63/s, the maximum compressive loads increase. When the strain rate increases from 0.63/s to 1.58/s, the increase of the maximum compressive loads becomes more significant. Correspondingly, the specimens under the strain rate of 1.58/s have greater maximum and residual compressive deformation than those under the strain rate of 0.63/s. However, under each strain rate, the surface roughness has little influences on the maximum load, maximum and residual deformation, as well as the interface age. Interestingly, under the strain rate of 1.58/s, the compressive load tends to increase more slowly with the increases in the surface roughness and interface age before the compressive load reaches the maximum value. There might be two reasons for the phenomenon. On the one hand, the increase in the surface roughness leads to an increase in the propagation time of stress waves at the interface, resulting in the compressive deformation increases more under the same compressive load and wave propagation velocity. On the other hand, the increase in the interface age induces more shrinkage stress at the interface. Before the compressive load achieves the maximum value, the interfacial tensile stress caused by the compressive load needs to counteract the effect of shrinkage stress, leading to the compressive load increases less under the same compressive deformation. However, the phenomenon is not significant when the strain rate reduces to 0.63 and 10^{-6}/s. It indicates that a lower strain rate can eliminate the influences of the surface roughness and interface age on the compressive load-deformation curves.

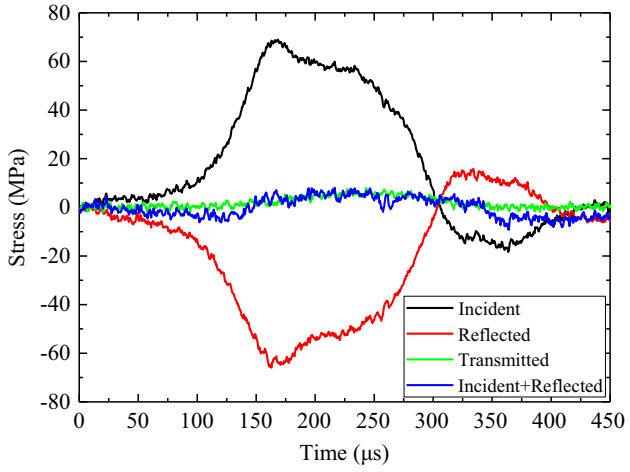

Fig. 4. Stress equilibrium check (SPR1A1V1-2).

3.3. Absorption energy

Fig. 7 shows the average absorption energy of specimens at two dynamic strain rates. The absorption energy of a specimen was calculated by the area under the compressive load-deformation curve shown in Fig. 6(b) and (c). Due to the compressive deformation in each quasi-static curve includes the compressive deformation of the two plywood strips, the absorption energy under the strain rate of 10^{-6}/s was not calculated.

It is obvious from Fig. 7 that specimens absorb more energy when the strain rate increases from 0.63/s to 1.58/s. With the increase in the absorption energy, the damage of specimens becomes more serious, especially the damage of old concrete substrates, as shown in Table 1. Under the strain rate of 0.63/s, the surface roughness and interface age have little effects on the absorption energy of specimens. When the strain rate rises up to 1.58/s, the absorption energy slightly reduces with the increases in the surface roughness and interface age. The reductions should be attributed to the phenomenon mentioned in Section 3.2. Due to the phenomenon, the stiffness of the ascending portion of the compressive load-deformation curve declines with the increases in the surface roughness and interface age. Meanwhile, the maximum load, maximum and residual deformation are almost unchanged. Hence, the area under the compressive load-deformation curve, i.e., the absorption energy, decreases.

3.4. Splitting tensile bond strength

Fig. 8 presents the average splitting tensile bond strength values of specimens at three strain rates. The quasi-static and dynamic splitting tensile bond strength were calculated by Eq. (2) and (8), respectively.

It is clear from Fig. 8 that the splitting tensile bond strength increases by 43%~51% when the strain rate increases from 10^{-6}/s

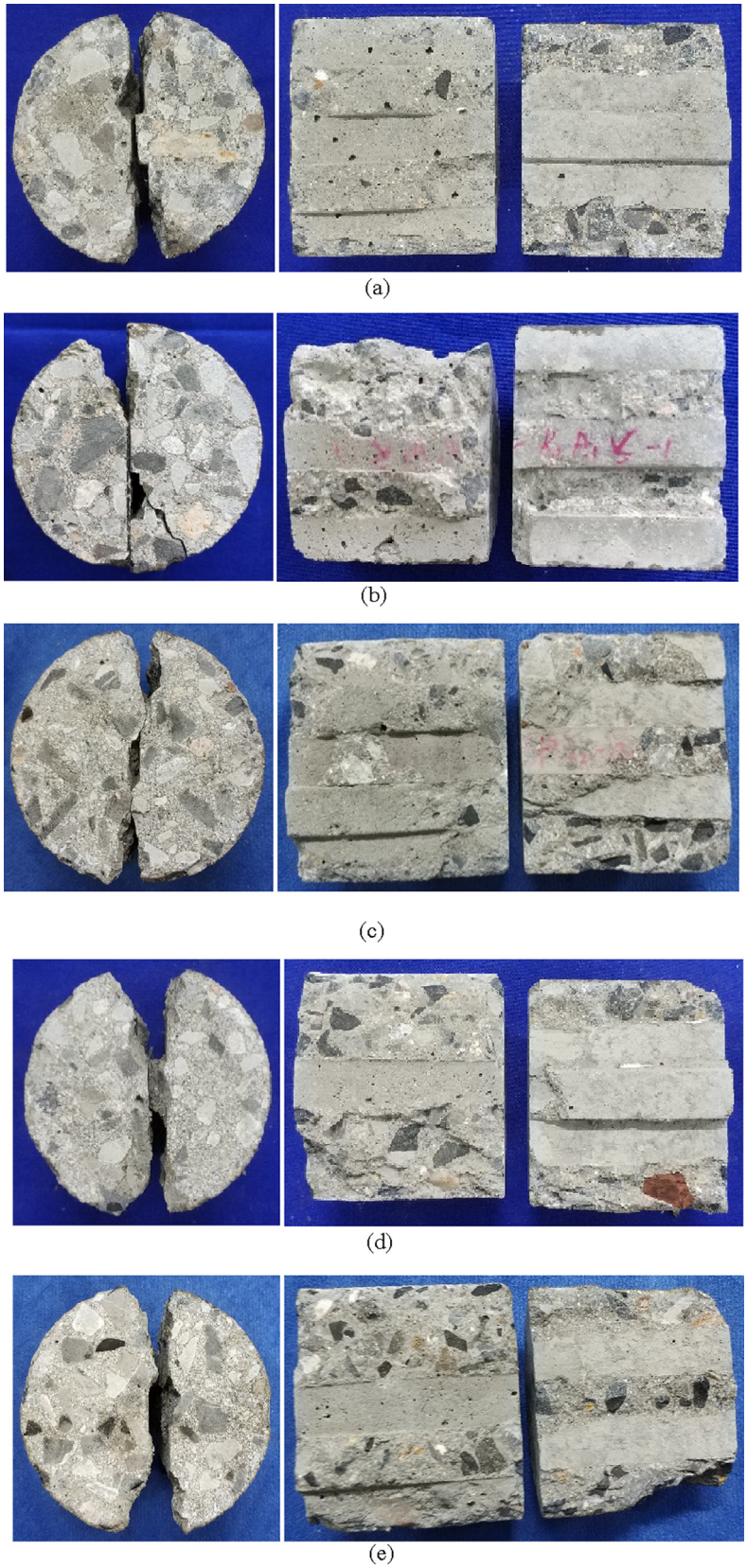

Fig. 5. Failure modes of splitting tensile specimens: (a) Ⅰ (SPR1A2V1-2); (b) Ⅱ (SPR1A1S-1); (c) III (SPR1A1V1-1); (d) IV (SPR2A2V2-3); and (e) V (SPR2A1V2-2). (Note: the new concrete semicylinder is on the left and the old concrete semicylinder is on the right in each figure.)

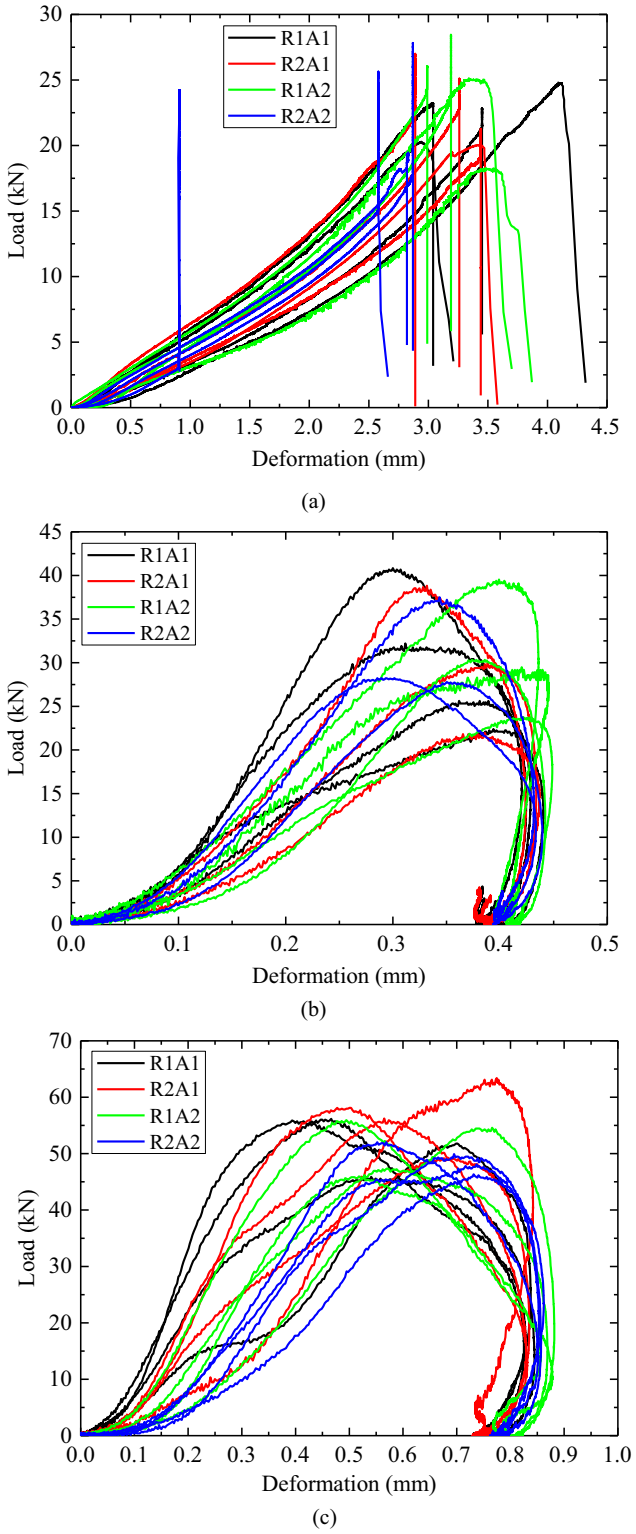

Fig. 6. Load-deformation curves of specimens: (a) under the strain rate of 10^{-6}/s; (b) under the strain rate of 0.63/s; and (c) under the strain rate of 1.58/s.

to 0.63/s. When the strain rate increases from 0.63/s to 1.58/s, the splitting tensile bond strength increases by 57%~88%. The strain-rate effect is significant. Note that the percentage increase for the specimens with the same surface roughness and interface age was obtained by dividing the strength difference between two strain rates by the strength at the smaller strain rate. Under the strain rates of 10^{-6} and 0.63/s, the surface roughness and interface age have no effects on the splitting tensile bond strength of specimens. When the strain rate is 1.58/s, the surface roughness and interface age also have little influences on the splitting tensile bond strength despite there are some fluctuations in results. These might be attributed to two reasons. On the one hand, failure modes in Fig. 5 shows that the old concrete substrate and new concrete layer of each specimen sustain more or less tensile damage at the interface. It means that the splitting tensile bond strength is related to the tensile strength of the old concrete substrate and new concrete layer, which depends on the compressive strength of old and new concrete, respectively. Table 2 shows that the cube compressive strength of old and new concrete is relatively close, indicating that the tensile strength of the old concrete substrate and new concrete layer is also close. Hence, regardless of the average roughness is 1.2 or 2.4 mm, the splitting tensile bond strength changes little. On the other hand, the interface ages in this experimental program, i.e., 60 and 120 days, are more than 28 days. At these ages, the tensile strength of old and new concrete is relatively stable. Thus, the splitting tensile bond strength almost no long increases when the interface age changes from 60 days to 120 days.

3.5. Dynamic increase factor of splitting tensile bond strength

As presented previously, the strain-rate effect is significant on the splitting tensile bond strength of concrete interfaces. Therefore, the dynamic increase factor of the splitting tensile bond strength is analyzed in this section. Due to the surface roughness and interface age have little influences on the splitting tensile bond strength, the effects of the two factors were not considered in the analysis. For the quasi-static splitting tensile bond strength, $f_{s,st}$, the average value of 3.16 MPa calculated by the test results of 16 specimens was employed. Then, the dynamic increase factors, DIF_{st}, of all the specimens were obtained by $f_{d,st}/f_{s,st}$. Note that the dynamic increase factor for a quasi-static specimen was equal to the ratio between the test result and the average value of 3.16 MPa. Fig. 9 (a) and (b) plot the relationships between DIF_{st} and the strain rate with linear–linear and linear-logarithmic scales, respectively. Clearly, DIF_{st} slowly increases when the strain rate is less than 0.44/s and quickly increases when the strain rate is beyond 0.44/s.

Unfortunately, so far, there is no formula to predict DIF_{st}. Hence, four existing formulas for the dynamic increase factor, DIF_t, of the tensile strength of concrete-like materials were collected and attempted to predict DIF_{st}.

Malvar and Ross [33] conducted a literature review to characterize strain-rate effects on the tensile strength of concrete and suggested a formula to estimate DIF_t as follows:

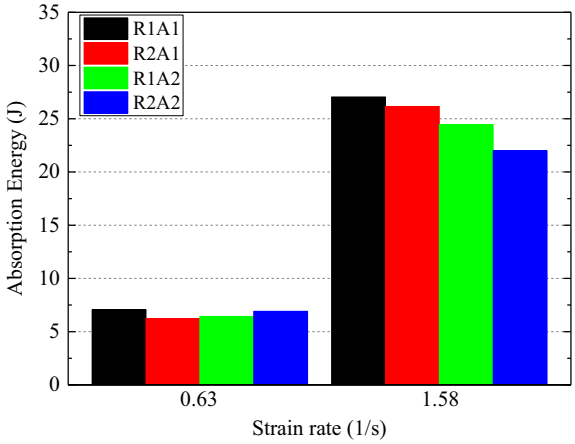

Fig. 7. Absorption energy at two dynamic strain rates.

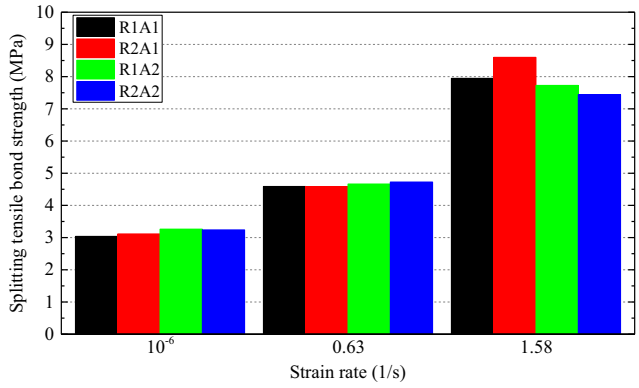

Fig. 8. Splitting tensile bond strength at three strain rates.

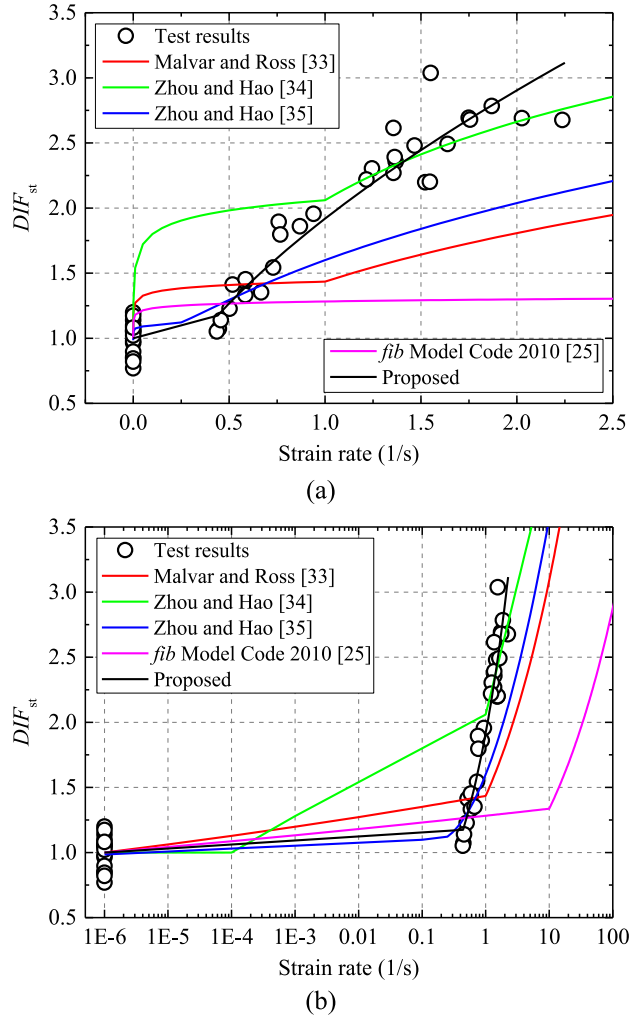

Fig. 9. Relationships between DIF_{st} and strain rate: (a) relationship with linear–linear scale; and (b) relationship with linear-logarithmic scale.

$$DIF_t = \frac{f_{d,t}}{f_{s,t}} = \begin{cases} \left(\frac{\dot{\varepsilon}}{10^{-6}}\right)^{\delta} & 10^{-6}/\mathrm{s} \leqslant \dot{\varepsilon} \leqslant 1.0/\mathrm{s} \\ \beta\left(\frac{\dot{\varepsilon}}{10^{-6}}\right)^{1/3} & \dot{\varepsilon} > 1.0/\mathrm{s} \end{cases} \tag{11}$$

where $f_{d,t}$ and $f_{s,t}$ are the dynamic and quasi-static tensile strength of concrete, respectively; and the coefficients δ and β are determined by $\delta = 1/(1+8f_c'/10)$ and $\lg\beta = 6\delta - 2$, respectively.

Through curve fitting from test results, Zhou and Hao [34] obtained a trilinear formula for DIF_t, which takes the following form

$$DIF_t = \frac{f_{d,t}}{f_{s,t}} = \begin{cases} 1 & \dot{\varepsilon} \leqslant 10^{-4}/\mathrm{s} \\ 2.06 + 0.26\lg\dot{\varepsilon} & 10^{-4}/\mathrm{s} < \dot{\varepsilon} \leqslant 1.0/\mathrm{s} \\ 2.06 + 2\lg\dot{\varepsilon} & \dot{\varepsilon} > 1.0/\mathrm{s} \end{cases} \tag{12}$$

On the basis of the experimental results of rock materials, Zhou and Hao [35] developed a bilinear formula for DIF_t, which is written as

$$DIF_t = \frac{f_{d,t}}{f_{s,t}} = \begin{cases} 0.0225\lg\dot{\varepsilon} + 1.12 & \dot{\varepsilon} \leqslant 0.1/\mathrm{s} \\ 0.7325(\lg\dot{\varepsilon})^2 + 1.235\lg\dot{\varepsilon} + 1.6 & 0.1/\mathrm{s} < \dot{\varepsilon} \leqslant 50/\mathrm{s} \end{cases} \tag{13}$$

By further determining the coefficients in Eq. (11), the fédération internationale du béton recommends a simplified formula for DIF_t in *fib* Model Code 2010 [25], which is given by

$$DIF_t = \frac{f_{d,t}}{f_{s,t}} = \begin{cases} \left(\frac{\dot{\varepsilon}}{10^{-6}}\right)^{0.018} & \dot{\varepsilon} \leqslant 10/\mathrm{s} \\ 0.0062\left(\frac{\dot{\varepsilon}}{10^{-6}}\right)^{1/3} & \dot{\varepsilon} > 10/\mathrm{s} \end{cases} \tag{14}$$

The predictions by the existing formulas are also shown in Fig. 9. Note that, for δ in Eq. (11), f_c' was taken as the average value of the strength of both old and new concrete in this analysis. It can be seen from Fig. 9 that, the transition strain rates, i.e., 1.0/s suggested by Malvar and Ross [33], 10^{-4} and 1.0/s proposed by Zhou and Hao [34], 0.1/s suggested by Zhou and Hao [35] and 10/s proposed by *fib* Model Code 2010 [25], are quite different from the experimental result of 0.44/s. When the strain rate is not more than 0.44/s, the predictions by Malvar and Ross [33] and *fib* Model Code 2010 [25] are higher than the experimental results. After the strain rate exceeds 0.44/s, the predictions by Malvar and Ross [33], Zhou and Hao [35] and *fib* Model Code 2010 [25] are lower than the experimental results. When the strain rate is more than 1.0/s, the predictions by Zhou and Hao [34] are close to the test results. However, before the strain rate achieves 1.0/s, the predictions by Zhou and Hao [34] are greater than the test results. Therefore, the existing formulas for DIF_t of the tensile strength of concrete-like materials cannot be used to predict DIF_{st} of the splitting tensile bond strength of concrete interfaces.

Consequently, a new formula for DIF_{st} is proposed as follows:

$$DIF_{st} = \frac{f_{d,st}}{f_{s,st}} = \begin{cases} 1.00 + 0.076 \times \frac{\dot{\varepsilon}}{10^{-6}} & 10^{-6}/\mathrm{s} \leqslant \dot{\varepsilon} \leqslant 0.44/\mathrm{s} \\ 0.0005\left(\frac{\dot{\varepsilon}}{10^{-6}}\right)^{0.60} & 0.44/\mathrm{s} < \dot{\varepsilon} \leqslant 2.24/\mathrm{s} \end{cases} \tag{15}$$

In the proposed formula, a bilinear dynamic increase factor-strain rate relationship is assumed. When the strain rate ranges from 0.44/s to 2.24/s, the expression is obtained by fitting the test data in this paper. When the strain rate ranges from 10^{-6}/s to 0.44/s, the dynamic increase factor-strain rate curve is assumed to be linear and then the corresponding expression is easily determined. The fitting curves of Eq. (15) with linear–linear and linear-logarithmic scales are plotted in Fig. 9(a) and (b), respectively. The coefficient of determination, R^2, of Eq. (15) is 0.94. It demonstrates that the proposed formula fits the test results well.

4. Conclusions

This paper experimentally investigated the quasi-static and dynamic splitting tensile bond behavior of new-to-old concrete interfaces. Influences of the strain rate, the surface roughness and the interface age on experimental results were presented. The experimental results contained failure modes, compressive

load-deformation curves, absorption energy and splitting tensile bond strength. In addition, the dynamic increase factor of the splitting tensile bond strength was analyzed. The main conclusions can be drawn as follows:

(1) When the average roughness increases from 1.2 mm to 2.4 mm, both the old concrete substrates and the new concrete layers sustain more tensile damage. When the interface age changes from 60 days to 120 days, the tensile damage of the old concrete substrates becomes more serious but that of the new concrete layers is almost unchanged. The splitting damage of the specimens under dynamic loading is not necessarily more serious than that under quasi-static loading. When the strain rate increases from 0.63/s to 1.58/s, the old concrete substrates undergo more tensile damage but the new concrete layers have similar tensile damage.

(2) Under a lower strain rate, i.e., 10^{-6} or 0.63/s, the surface roughness and interface age have little influences on the compressive load-deformation curves. However, when the strain rate increases to 1.58/s, the compressive load increases more slowly with the increases in the surface roughness and interface age before the compressive load reaches the maximum value. This phenomenon results in slight reductions of the absorption energy with the increases in the surface roughness and interface age.

(3) When the strain rate increases from 10^{-6}/s to 0.63/s, the splitting tensile bond strength increases by 43%~51%. When the strain rate increases from 0.63/s to 1.58/s, the splitting tensile bond strength increases by 57%~88%. These indicates that the strain-rate effect is significant. However, the surface roughness and interface age have little effects on the splitting tensile bond strength.

(4) Existing formulas for the dynamic increase factor of the tensile strength of concrete-like materials cannot be used to predict the dynamic increase factor of the splitting tensile bond strength of concrete interfaces. Hence, a new formula, which is fitted from the test date in this experimental program, is proposed for concrete interfaces. It should be noted that for concrete interfaces where old and new concrete has different properties from that used in this paper, the applicability of this new formula needs to be further verified.

As mentioned in Introduction, there are many factors affecting the splitting tensile bond behavior of new-to-old concrete interfaces. The range of each factor may also have an important effect on the interfacial behavior. Thus, future work can focus on the influences of the difference of strength grades between old and new concrete, the difference of stiffness between old and new concrete, and the early ages of concrete interfaces on the interfacial dynamic splitting tensile bond behavior. Besides, the effects of higher strain rates should also be considered since a significant strain-rate effect has been observed. Note that under a higher loading rate, it is very crucial to ensure the old concrete substrate and new concrete layer are not severely damaged when the concrete interface is split.

CRediT authorship contribution statement

Bo Hu: Conceptualization, Methodology, Validation, Supervision, Writing - review & editing. **Teng-Fei Meng:** Data curation, Software, Writing - original draft. **Yuan Li:** Data curation, Software, Validation. **Dao-Zhong Li:** Investigation, Resources. **Long Chen:** Resources.

Declaration of Competing Interest

The authors declare that they have no known competing financial interests or personal relationships that could have appeared to influence the work reported in this paper.

Acknowledgments

The financial support of this work from the National Natural Science Foundation of China under Grant No. 51408175 is greatly appreciated. The authors also wish to thank Dr. Yan Liu from Hefei Hengjia Mechanical and Electrical Equipment Company Limited and Dr. Xu-Tao Wu from Hefei University of Technology for their assistance during the test program.

References

[1] M. Kuroda, T. Watanabe, N. Terashi, Increase of bond strength at interfacial transition zone by the use of fly ash, Cem. Concr. Res. 30 (2) (2000) 253–258.
[2] A. Momayez, M.R. Ehsani, A.A. Ramezanianpour, H. Rajaie, Comparison of methods for evaluating bond strength between concrete substrate and repair materials, Cem. Concr. Res. 35 (4) (2005) 748–757.
[3] G. Li, A new way to increase the long-term bond strength of new-to-old concrete by the use of fly ash, Cem. Concr. Res. 33 (6) (2003) 799–806.
[4] E.N.B.S. Júlio, F.A.B. Branco, V.D. Silva, Concrete-to-concrete bond strength. Influence of the roughness of the substrate surface, Constr. Build. Mater. 18 (9) (2004) 675–681.
[5] E.N.B.S. Júlio, F.A.B. Branco, V.D. Silva, Concrete-to-concrete bond strength: influence of an epoxy-based bonding agent on a roughened substrate surface, Mag. Concr. Res. 57 (8) (2005) 463–468.
[6] E. Bonaldo, J.A.O. Barros, P.B. Lourenço, Bond characterization between concrete substrate and repairing SFRC using pull-off testing, Int. J. Adhes. Adhes. 25 (6) (2005) 463–474.
[7] P.M.D. Santos, E.N.B.S. Júlio, V.D. Silva, Correlation between concrete-to-concrete bond strength and the roughness of the substrate surface, Constr. Build. Mater. 21 (8) (2007) 1688–1695.
[8] H. Huang, B. Liu, K. Xi, T. Wu, Interfacial tensile bond behavior of permeable polymer mortar to concrete, Constr. Build. Mater. 121 (2016) 210–221.
[9] Y. He, X. Zhang, R.D. Hooton, X. Zhang, Effects of interface roughness and interface adhesion on new-to-old concrete bonding, Constr. Build. Mater. 151 (2017) 582–590.
[10] D.P. Bentz, I. De la Varga, J.F. Muñoz, R.P. Spragg, B.A. Graybeal, D.S. Hussey, D. L. Jacobson, S.Z. Jones, J.M. LaManna, Influence of substrate moisture state and roughness on interface microstructure and bond strength: Slant shear vs. pull-off testing, Cem. Concr. Comp. 87 (2018) 63–72.
[11] J. Qin, J. Qian, C. You, Y. Fan, Z. Li, H. Wang, Bond behavior and interfacial micro-characteristics of magnesium phosphate cement onto old concrete substrate, Constr. Build. Mater. 167 (2018) 166–176.
[12] S.H. Abo Sabah, M.H. Hassan, N. Muhamad Bunnori, M.A. Megat Johari, Bond strength of the interface between normal concrete substrate and GUSMRC repair material overlay, Constr. Build. Mater. 216 (2019) 261–271.
[13] K. Gadri, A. Guettala, Evaluation of bond strength between sand concrete as new repair material and ordinary concrete substrate (The surface roughness effect), Constr. Build. Mater. 157 (2017) 1133–1144.
[14] G. Xiong, J. Liu, G. Li, H. Xie, A way for improving interfacial transition zone between concrete substrate and repair materials, Cem. Concr. Res. 32 (12) (2002) 1877–1881.
[15] A.D. Espeche, J. León, Estimation of bond strength envelopes for old-to-new concrete interfaces based on a cylinder splitting test, Constr. Build. Mater. 25 (3) (2011) 1222–1235.
[16] P.M.D. Santos, E.N.B.S. Júlio, Factors affecting bond between new and old concrete, ACI Mater. J. 108 (4) (2011) 449–456.
[17] B.A. Tayeh, B.H. Abu Baka, M.A. Megat Johari, Y.L. Voo, Mechanical and permeability properties of the interface between normal concrete substrate and ultra high performance fiber concrete overlay, Constr. Build. Mater. 36 (2012) 538–548.
[18] B.A. Tayeh, B.H. Abu Bakar, M.A. Megat Johari, Characterization of the interfacial bond between old concrete substrate and ultra high performance fiber concrete repair composite, Mater. Struct. 46 (5) (2013) 743–753.
[19] H. Costa, R.N.F. Carmo, E. Julio, Influence of lightweight aggregates concrete on the bond strength of concrete-to-concrete interfaces, Constr. Build. Mater. 180 (2018) 519–530.
[20] S. Xu, F. Mu, J. Wang, W. Li, Experimental study on the interfacial bonding behaviors between sprayed UHTCC and concrete substrate, Constr. Build. Mater. 195 (2019) 638–649.
[21] S. Gao, X. Zhao, J. Qiao, Y. Guo, G. Hu, Study on the bonding properties of Engineered Cementitious Composites (ECC) and existing concrete exposed to high temperature, Constr. Build. Mater. 196 (2019) 330–344.
[22] H. Huang, Y. Yuan, W. Zhang, Z. Gao, Bond behavior between lightweight aggregate concrete and normal weight concrete based on splitting-tensile test, Constr. Build. Mater. 209 (2019) 306–314.
[23] S. Gao, J. Jin, G. Hu, L. Qi, Experimental investigation of the interface bond properties between SHCC and concrete under sulfate attack, Constr. Build. Mater. 217 (2019) 651–663.
[24] B. Hu, Y. Li, Y. Liu, Dynamic slant shear bond behavior between new and old concrete, Constr. Build. Mater. 238 (2020) 117779.
[25] fib Bulletin 55. Model Code 2010, First complete draft, Volume 1. fib – fédération internationale du béton, International Federation for Structural Concrete, Lausanne, 2010.

[26] GB 50666-2011. Code for construction of concrete structures. Ministry of Housing and Urban-Rural Development of the People's Republic of China, Beijing, 2012. (in Chinese).
[27] JGJ 1-2014. Technical specification for precast concrete structures. Ministry of Housing and Urban-Rural Development of the People's Republic of China, Beijing, 2014. (in Chinese)
[28] GB 50367-2013. Code for design of strengthening concrete structure. Ministry of Housing and Urban-Rural Development of the People's Republic of China, Beijing, 2013. (in Chinese).
[29] JGJ 55-2011. Specification for mix proportion design of ordinary concrete. Ministry of Housing and Urban-Rural Development of the People's Republic of China, Beijing, 2011. (in Chinese).
[30] GB/T 50081-2002. Standard for test method of mechanical properties on ordinary concrete. Ministry of Housing and Urban-Rural Development of the People's Republic of China, Beijing, 2003. (in Chinese).
[31] Y.B. Lu, Q.M. Li, About the dynamic uniaxial tensile strength of concrete-like materials, Int. J. Impact Eng. 38 (2011) 171–180.
[32] ACI 318M-05. Building code requirement for structural concrete and commentary. American Concrete Institute, Farmington Hills, 2005.
[33] L.J. Malvar, C.A. Ross, Review of strain rate effects for concrete in tension, ACI Mater. J. 95 (6) (1998) 735–739.
[34] X.Q. Zhou, H. Hao, Mesoscale modelling of concrete tensile failure mechanism at high strain rates, Comput. Struct. 86 (2008) 2013–2026.
[35] X.Q. Zhou, H. Hao, Modelling of compressive behaviour of concrete-like materials at high strain rate, Int. J. Solids Struct. 45 (2008) 4648–4661.